ARTICLE

Longitudinal cognitive and biomarker changes in dominantly inherited Alzheimer disease

Eric McDade, DO, Guoqiao Wang, PhD, Brian A. Gordon, PhD, Jason Hassenstab, PhD, Tammie L.S. Benzinger, MD, Virginia Buckles, PhD, Anne M. Fagan, PhD, David M. Holtzman, MD, Nigel J. Cairns, PhD, Alison M. Goate, PhD, Daniel S. Marcus, PhD, John C. Morris, MD, Katrina Paumier, PhD, Chengjie Xiong, PhD, Ricardo Allegri, MD, Sarah B. Berman, MD, William Klunk, MD, James Noble, MD, John Ringman, MD, Bernardino Ghetti, MD, Martin Farlow, MD, Reisa A. Sperling, MD, Jasmeer Chhatwal, MD, Stephen Salloway, MD, Neill R. Graff-Radford, MD, Peter R. Schofield, MD, Colin Masters, MD, Martin N. Rossor, MD, Nick C. Fox, MD, Johannes Levin, MD, Mathias Jucker, PhD, and Randall J. Bateman, MD, for the Dominantly Inherited Alzheimer Network

Correspondence
Dr. McDade
ericmcdade@wustl.edu
or Dr. Bateman
batemanr@wustl.edu

Neurology® 2018;91:e1295-e1306. doi:10.1212/WNL.0000000000006277

Abstract

Objective
To assess the onset, sequence, and rate of progression of comprehensive biomarker and clinical measures across the spectrum of Alzheimer disease (AD) using the Dominantly Inherited Alzheimer Network (DIAN) study and compare these to cross-sectional estimates.

Methods
We conducted longitudinal clinical, cognitive, CSF, and neuroimaging assessments (mean of 2.7 [±1.1] visits) in 217 DIAN participants. Linear mixed effects models were used to assess changes in each measure relative to individuals' estimated years to symptom onset and to compare mutation carriers and noncarriers.

Results
Longitudinal β-amyloid measures changed first (starting 25 years before estimated symptom onset), followed by declines in measures of cortical metabolism (approximately 7–10 years later), then cognition and hippocampal atrophy (approximately 20 years later). There were significant differences in the estimates of CSF p-tau$_{181}$ and tau, with elevations from cross-sectional estimates preceding longitudinal estimates by over 10 years; further, longitudinal estimates identified a significant decline in CSF p-tau$_{181}$ near symptom onset as opposed to continued elevations.

Conclusion
These longitudinal estimates clarify the sequence and temporal dynamics of presymptomatic pathologic changes in autosomal dominant AD, information critical to a better understanding of the disease. The pattern of biomarker changes identified here also suggests that once β-amyloidosis begins, additional pathologies may begin to develop less than 10 years later, but more than 15 years before symptom onset, an important consideration for interventions meant to alter the disease course.

MORE ONLINE

CME Course
NPub.org/cmelist

From the Department of Neurology (E.M., J.H., V.B., A.M.F., D.M.H., J.C.M., K.P., R.J.B.), Division of Biostatistics (G.W., C.X.), Department of Radiology (B.A.G., T.L.S.B., D.S.M.), and Department of Pathology (N.J.C.), Washington University School of Medicine, Saint Louis, MO; Department of Neuroscience (A.M.J.), Icahn School of Medicine at Mount Sinai, New York, NY; Fundación para la Lucha contra las Enfermedades Neurológicas de la Infancia (FLENI) (R.A.), Instituto de Investigaciones Neurológicas Raúl Correa, Buenos Aires, Argentina; University of Pittsburgh School of Medicine (S.B.B., W.K.), PA; College of Physicians and Surgeons (J.N.), Columbia University, New York, NY; Department of Neurology (J.R.), Keck School of Medicine of University of Southern California, Los Angeles; Department of Neurology (B.G., M.F.), Indiana University, Indianapolis; Massachusetts General Hospital (R.A.S., J.C.), Harvard Medical School, Boston; Butler Hospital and Brown University (S.S.), Providence, RI; Department of Neurology (N.R.G.-R.), Mayo Clinic Jacksonville, FL; Neuroscience Research Australia (P.R.S.); School of Medical Sciences (P.R.S.), University of New South Wales, Sydney; The Florey Institute and the University of Melbourne (C.M.), Parkville, Australia; Dementia Research Centre, Institute of Neurology (M.N.R., N.C.F.), University College London, UK; German Center for Neurodegenerative Diseases (DZNE) Munich (J.L.); Department of Neurology (J.L.), Ludwig-Maximilians Universität München; German Center for Neurodegenerative Diseases (DZNE) Tübingen (M.J.); and Hertie-Institute for Clinical Brain Research (M.J.), University of Tübingen, Germany.

Go to Neurology.org/N for full disclosures. Funding information and disclosures deemed relevant by the authors, if any, are provided at the end of the article.

Coinvestigators are listed at links.lww.com/WNL/A698.

Glossary

Aβ = β-amyloid; **AD** = Alzheimer disease; **ADAD** = autosomal dominant Alzheimer disease; **aMC** = asymptomatic mutation carriers; **CDR** = Clinical Dementia Rating scale; **DIAN** = Dominantly Inherited Alzheimer Network; **EYO** = estimated years to symptom onset; **FDG** = fluorodeoxyglucose; **LME** = linear mixed effects model; **LOAD** = late-onset Alzheimer disease; **MC** = mutation carriers; **NC** = noncarriers; **NFT** = neurofibrillary tangle; **p-tau** = phosphorylated tau; **PiB** = Pittsburgh compound B.

Cross-sectional data from the Dominantly Inherited Alzheimer Network (DIAN) and other populations of autosomal dominant Alzheimer disease (ADAD) have identified a relatively consistent pattern of biomarker and clinical change spanning the decades before and after expected symptom onset.[1–7] Cross-sectional studies provide critical information to inform our understanding of the general pattern of biomarker changes relative to clinical symptoms[8–11] and provide support for proposed models in both ADAD and sporadic late-onset Alzheimer disease (LOAD).[12]

The predictability of symptom onset in ADAD facilitates longitudinal studies of the presymptomatic period by enabling the study of rates of change and temporal ordering of biomarker changes relative to the onset of dementia.[13] With increasing emphasis on prevention trials in Alzheimer disease (AD), characterization of preclinical pathologic changes is critical.[2,14,15] However, the longitudinal rates and order of different biomarker, cognitive, and clinical measures have not been evaluated comprehensively in a large, well-controlled study.

Our previous analysis of the disease trajectory has been highly informative in estimating the pattern of disease onset, but was based on cross-sectional data.[1] Such data are influenced by intersubject variability. Longitudinal data attenuate this and therefore provide more accurate information regarding the onset and course of changes over time. Here, we assessed the longitudinal pattern of changes in key imaging, CSF, cognitive, and clinical outcomes across the ADAD disease spectrum. We sought to (1) report the first longitudinal results of clinical, cognitive, and biomarker changes in DIAN across the disease spectrum and (2) compare results from longitudinal vs cross-sectional assessments to better understand the course of the disease.

Methods

Study design

Participants with at least 50% risk of inheriting an ADAD mutation from families with a confirmed genetic mutation in *PSEN1*, *PSEN2*, or *APP* were enrolled. At each study visit, participants underwent clinical assessments, cognitive testing, neuroimaging, and CSF studies. The details of study structure and assessments can be found in prior publications.[1,16] In summary, follow-up intervals were determined by clinical status (normal or impaired) of each participant and by the estimated years to symptom onset (EYO): visits were annual for symptomatic participants and asymptomatic participants within (before or after) 3 years of their EYO and every 3 years for asymptomatic participants more than 3 years before EYO. Data were obtained from quality controlled data (January 26, 2009–June 30, 2015) and included all 411 participants with baseline evaluations, 217 of whom had at least one follow-up visit during this period. The presence or absence of an ADAD mutation was determined using PCR-based amplification of the appropriate exon followed by Sanger sequencing.

Standard protocol approvals, registrations, and patient consents

The study protocol received approval by the institutional review boards of all participating sites. The DIAN study is performed in accordance with the Declaration of Helsinki and written informed consent was obtained from each participant.

Clinical assessments

Standardized clinical evaluations, including a study partner, was performed for each participant. The Clinical Dementia Rating scale (CDR) was used to indicate dementia stage. Participants were rated as cognitively normal (CDR = 0), very mild dementia (CDR = 0·5), mild dementia (CDR = 1), or moderate dementia (CDR = 2).[17] Evaluating clinicians were blind to genetic status and all biomarker results.

Estimated years to symptom onset

Symptom risk in DIAN is defined by EYO. EYO was defined as follows: a parental age at earliest symptom onset was established for each participant by semi-structured interview. The parental age at onset for each mutation was then entered into a database consisting of the combined symptom onset values from DIAN and from prior publications from ADAD cohorts to determine an average age at onset specific to each mutation.[13] Using this mutation-specific age at onset, each participant's age at the time of clinical assessment was subtracted to define the mutation EYO. When a specific mutation average age at onset was unknown, the parental or proxy age at onset was used to define EYO.[13] For participants who were symptomatic at baseline, as assessed by a CDR >0, the reported age at actual symptom onset was subtracted from age at each clinical assessment to define EYO.

Neuropsychological assessments

A comprehensive neuropsychological battery assessing general cognitive function, memory, attention, executive function, visuospatial function, and language was performed at each visit.[11] From these tests we developed a cognitive composite that reliably detects decline across the range of EYO and CDR.[18] The composite represents the average of

the z scores from tests including episodic memory, complex attention, and processing speed, and a general cognitive screen (Mini-Mental State Examination) (e-Methods, doi.org/10.5061/dryad.f6sj385).

Brain imaging

The complete MRI [C-11] Pittsburgh compound B (PiB) PET and metabolic imaging with [F-18] fluorodeoxyglucose (FDG-PET) acquisition and imaging processing is detailed in previous publications.[19] A neocortical standardized uptake value ratio was used to determine levels of precuneus β-amyloid (Aβ) deposition and a precuneus region of interest for FDG metabolism, using cerebellar gray matter as the reference region and applying partial volume correction using a regional point spread function as previously described for PiB-PET.[20] We chose a single precuneus (average of both hemispheres) region for FDG based on prior work in this and other ADAD cohorts indicating this region as the earliest effected by a number of different imaging measures.[3,5,19] The corresponding structural MRI was used at each visit for registration of the PiB-PET. We have previously demonstrated that for PiB-PET there were no significant differences in results when using a cerebellar, pons, or white matter reference.[21]

CSF collection and analyses

Aβ1-42, total tau, and tau phosphorylated at threonine 181 ($p\text{-tau}_{181}$) were measured by immunoassay (INNO-BIA AlzBio3; Innogenetics, Gent, Belgium). In order to limit methodologic variability, a single immunoassay lot number was used, and longitudinal samples from a given individual were run on the same assay plate.

Statistical analyses

Demographic characteristics were compared between mutation carriers (MC) and noncarriers (NC) using 2-sample t tests or Pearson χ^2 tests.

Rate of change

Individual estimates

The best linear unbiased estimators of the individual's rate of change over the follow-up was estimated using general linear mixed effects model (LME) and then were plotted against baseline EYO using local regression (LOESS)[22] (figure 1) only for those participants with at least 2 measurements. Based on the LOESS curves, we then determined the most appropriate pattern of change across the total baseline EYO period for each variable using the goodness-of-fit Akaike information criterion, e.g., linear with a change point (spline) (model A), linear (model B), no association (model C), or quadratic data (e-Methods, table e-1, doi.org/10.5061/dryad.f6sj385). Finally, if the linear spline model or the quadratic model is selected, we test the significance of the quadratic term or the line spline term in the model. If the test achieves significance, we use that as the final model, otherwise we drop that term and use what left as the final model. *APOE* allele genotype was not included since there were no significant differences in outcomes by *APOE* status.

Groupwise estimates

The optimal models identified for each outcome were then used for the groupwise estimates and included any participant with at least one measurement. For each outcome, we evaluated (1) the association between the rate of change and baseline EYO; (2) the baseline EYO point where the rate of change became significantly different between MCs and NCs; (3) the baseline EYO point where the significant difference occurred cross-sectionally between MCs and NCs. We repeated each analysis for asymptomatic MCs also to assess whether the rate of change estimates were overly influenced by the symptomatic population. For model C, fixed effects included sex, time since baseline, mutation group (carriers vs noncarriers), and baseline EYO; random effects included random intercepts for each family to account for the family cluster correlation, random intercepts, and slopes for each individual with unstructured covariance matrix to account for correlation among repeated measures. When the association between baseline EYO and the rate of change is modeled using models A and B, the same fixed effects and random effects as in model C were used, plus all possible 2- or 3-way interactions among baseline EYO, mutation group, and follow-up time were included in the model to estimate the rate of change and mean of each outcome at each EYO point.

To visualize the differences in the estimated longitudinal change vs cross-sectional change, 5-year intervals of longitudinal change estimated using the LMEs was plotted with 5-year intervals of cross-sectional change estimated using a LOESS against baseline EYO. Finally, to visualize the order and magnitude of the rate of change over EYO for all outcomes together, we converted each to z scores using the mean and the SD values for all MCs and NCs. Each participant's z score rate of change was estimated using LME models and plotted in one figure using LOESS.

All p values were based on 2-sided tests and values <0.05 were considered significant. All analyses were conducted using SAS 9.4 (SAS Institute Inc., Cary, NC). All missing data were considered missing at random. The model accuracy for each step of the analyses was evaluated to ensure no violations of the underlying assumptions for the methods used.

Data availability

All data used in the preparation of this manuscript are available upon request to qualified researchers. Information can be found at dian.wustl.edu/our-research/observational-study/dian-observational-study-investigator-resources/data-request-terms-and-instructions/.

Results

Study participants

We analyzed 411 individuals (217 with repeated visits) from the DIAN cohort (table 1). Of the MC, 197 (78.5%) had *PSEN1*, 20 (7.9%) *PSEN2*, and 34 (13.5%) *APP* mutations

Figure 1 Individual longitudinal imaging, CSF, and clinical measures over estimated year to symptom onset (EYO) for mutation carriers and noncarriers

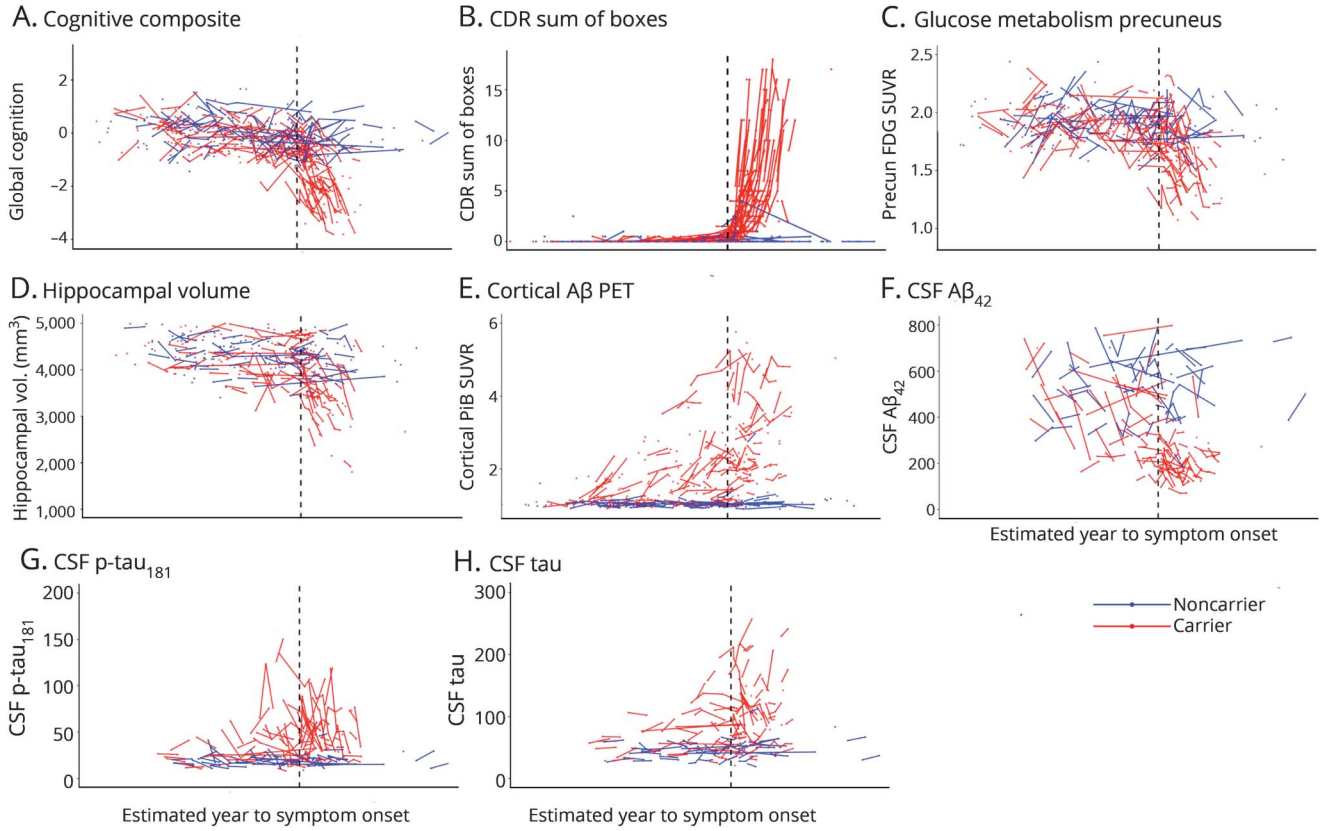

(A–H) Individual longitudinal changes for all CSF, imaging, and clinical biomarkers for mutation carriers (red) and noncarriers (blue). To maintain blinding of genetic status, the values of the x-axis (EYO) have been removed. The black vertical line represents the point of estimated symptom onset. Aβ = β-amyloid; CDR = Clinical Dementia Rating scale; FDG = fluorodeoxyglucose; p-tau = phosphorylated tau; PiB = Pittsburgh compound B; SUVR = standardized uptake value ratio.

and 56.9% were asymptomatic at baseline (CDR 0). The mean (SD) estimated age at onset of symptoms was 47.20 (7.1) years. The number of individuals with longitudinal assessments varied by the different outcomes (i.e., CSF vs clinical) and ranged from 121 to 217 (table 2) with a mean follow-up over 2 years (figure 1).

Longitudinal rates of change

Estimates of individual rates of change over baseline EYO in MC and NC

In MC, there was no association between the rate of change and baseline EYO for CSF tau (figure 2H), relatively linear associations for precuneus-FDG, PiB, and CSF $A\beta_{42}$ (figures 2, C, E and F), and linear association with 2 splines (2 different linear phases) for the cognitive composite, CDR sum of boxes, CSF p-tau, and hippocampal volumes (figure 2, A, B, D, and G), indicating different rates of change at different stages of the disease. The goodness-of-fit indices suggested a change point at baseline −7 EYO for CSF p-tau, −4 EYO for cognitive composite, −3 EYO for hippocampal volumes, and −1 EYO for CDR sum of boxes (figure e-1 and table e-1, doi.org/10.5061/dryad.f6sj385). Table 3 provides the estimate for each measure associated with time in the model with *p* values for the spline in EYO indicating the existence of the change points: the estimates for each outcome are shown for the asymptomatic MCs (aMCs) only and for all MCs (CDR 0 and greater). Table e-2 (doi.org/10.5061/dryad.f6sj385) provides the annual EYO estimates for the rate of change for each biomarker from as early as −25 to +10 within MC and between MC and NC.

Over EYO, Aβ demonstrated the earliest detectable change, beginning at least 25 years before estimated symptom onset (table 4). Between the 2 measures of Aβ, fibrillar amyloid continuously increased across EYO (annual mean percent change) (6.1%), and CSF$A\beta_{42}$ demonstrated a decrease in rate of change (−8.8%) that slowed near symptom onset (table e-2, doi.org/10.5061/dryad.f6sj385) (figure 2). Less than 10 years after the start of Aβ change, there was evidence of a decline in precuneus metabolism at −17 EYO (−1.16%). Following metabolic changes, CSF p-tau declined at −3 EYO (−9.7%), cognition also declined at −3 EYO (−0.08 standard units), hippocampal atrophy accelerated at −2 EYO (−1.4%), and CDR sum of boxes increased at 0 (0.64 boxes). Both CSF tau and p-tau in MCs showed significantly higher levels

Table 1 Characteristics of the study participants at baseline

All participants	Carriers (n = 251)	Noncarriers (n = 160)	*p* Value[a]
Age, y, mean (SD)	39.1 (11.1)	39.6 (11.5)	0.71
Female, n (%)	139 (55.4)	95 (59.4)	0.43
Education, y, mean (SD)	14.2 (3.1)	14.6 (2.9)	0.16
CDR >0, n (%)	101 (40.2)	11 (6.9)	<0.0001
CDR 0, n (%)	150 (59.8)	149 (93.1)	
APOE ε4 carrier, n (%)	73 (29.1)	45 (28.1)	0.83
CSF Aβ42, pg/mL, mean (SD)	334.9 (179)	546.6 (143)	<0.0001
CSF p-tau$_{181}$, pg/mL, mean (SD)	48.9 (28.9)	22.5 (7.1)	<0.0001
CSF tau, pg/mL, mean (SD)	93.9 (47.1)	48.1 (15.5)	<0.0001
Amyloid PET global SUVR, mean (SD)	2.01 (1.04)	1.06 (0.16)	<0.0001
FDG PET precuneus SUVR, mean (SD)	1.82 (0.22)	1.90 (0.16)	<0.0001
Hippocampal volume, mm^3, mean (SD)	4,124 (640)	4,369 (396)	<0.0001
DIAN cognitive composite, mean (SD)	−0.69 (1.06)	−0.03 (0.60)	<0.0001
EYO, mean (SD)	−7.9 (10.9)	−8.9 (11.7)	0.36

Longitudinal participants only	Carriers (n = 142)	Noncarriers (n = 75)	*p* Value[a]
Age, y, mean (SD)	40.6 (10.9)	40.4 (11.1)	0.88
Female, n (%)	84 (59.2)	49 (65.3)	0.37
Education, y, mean (SD)	14.0 (2.9)	14.5 (2.5)	0.15
CDR >0, n (%)	68 (47.9)	6 (8.0)	<0.0001
CDR 0, n (%)	74 (52.1)	69 (92.0)	
APOE ε4 carrier, n (%)	43 (30.3)	18 (24.0)	0.33
CSF Aβ42, pg/mL, mean (SD)	334.9 (179)	546.6 (143)	<0.0001
CSF p-tau$_{181}$, pg/mL, mean (SD)	48.9 (28.9)	22.5 (7.1)	<0.0001
CSF tau, pg/mL, mean (SD)	93.9 (47.1)	48.1 (15.5)	<0.0001
Amyloid PET global SUVR, mean (SD)	2.10 (1.07)	1.07 (0.22)	<0.0001
FDG PET precuneus SUVR, mean (SD)	1.79 (0.24)	1.90 (0.02)	0.0001
Hippocampal volume, mm^3, mean (SD)	4,033 (600)	4,366 (393)	<0.0001
DIAN cognitive composite, mean (SD)	−0.87 (0.09)	0.05 (0.61)	<0.0001
EYO, mean (SD)	−6.0 (10.0)	−7.6 (11.6)	0.29

Mutation carriers only	CDR 0 (n = 150)	CDR >0 (n = 101)	*p* Value
Age, y, mean (SD)	34.4 (9.1)	46.1 (10.0)	<0.0001
Female, n (%)	84 (56.0)	55 (54.5)	0.70
Education, y, mean (SD)	14.7 (3.0)	13.3 (3.1)	0.0009
APOE ε4 carrier, n (%)	40 (26.7)	33 (32.7)	0.26
CSF Aβ42, pg/mL, mean (SD)	431 (187)	230.8 (92)	<0.0001
CSF p-tau$_{181}$, pg/mL, mean (SD)	43.0 (29.8)	55.4 (27.0)	0.025
CSF tau, pg/mL, mean (SD)	73.6 (34.5)	115.9 (49.3)	<0.0001

Continued

Table 1 Characteristics of the study participants at baseline *(continued)*

Mutation carriers only	CDR 0 (n = 150)	CDR >0 (n = 101)	*p* Value
Amyloid PET global SUVR, mean (SD)	1.67 (0.76)	2.76 (1.18)	<0.0001
FDG PET precuneus SUVR, mean (SD)	1.89 (0.17)	1.68 (0.250)	<0.0001
Hippocampal volume, mm^3, mean (SD)	4,406 (495)	3,733 (615)	<0.0001
DIAN cognitive composite, mean (SD)	−0.11 (0.6)	−1.67 (0.9)	<0.0001
EYO, mean (SD)	−13.6 (9.1)	0.64 (7.1)	<0.0001

Abbreviations: Aβ = β-amyloid; CDR = Clinical Dementia Rating scale; DIAN = Dominantly Inherited Alzheimer Network; EYO = estimated years to symptom onset; FDG = fluorodeoxyglucose; p-tau = phosphorylated tau; SUVR = standardized uptake value ratio.
[a] *p* Values were calculated without taking into account the family cluster correlation and were similar to those calculated using mixed effects models to account for the family cluster correlation.

compared to NCs at −14 and −11 EYO, respectively, but only in cross-sectional analyses.

In general, the estimated rates of change were greater when including all MCs, with the exception of CSF tau and p-tau, which demonstrated a positive rate of change nearly 3 times greater for the aMCs (not statistically significant) relative to the estimates for all MCs. This suggested a greater rate of elevation of soluble tau measures prior to the onset of symptoms and a decline with the onset of cognitive decline (table 3), whereas with most other variables the estimated rates of change remained in the same direction over the course of the disease. Importantly, the mean to SD ratio for both tau measures was the largest of all the variables that decreases the sensitivity for identifying longitudinal change. For NCs, there was evidence of an increase in precuneus FDG from −25 to −14 EYO (table e-2, doi.org/10.5061/dryad.f6sj385). Otherwise, no other annual rates of change for any biomarker in NCs were different from zero over EYO.

To visualize the order and rate of change over EYO for all variables together, each individual's standardized values were then used to estimate an annualized rate of change across the EYO (figure e-2, doi.org/10.5061/dryad.f6sj385) that was comparable between outcomes. In the figure, the mark on each line indicates the EYO point when the rate of change for that measure was statistically different between MCs and NCs as defined above.

Longitudinal and cross-sectional estimates of change in MC and NC

To compare the predicted change based on the longitudinal data with those based on cross-sectional data, the analyses were repeated to determine the EYO point where the means of each outcome at baseline (cross-sectional estimates) for all MCs first became statistically significant compared with NCs. We found that the order of change was relatively similar between longitudinal and cross-sectional estimates, particularly for amyloid PET, FDG PET, and hippocampal volumes (table 2). Yet, there were large differences in the EYO point of change (more than 10 years) for CSF measures in longitudinal vs cross-sectional estimates. Further, the longitudinal rates of change were different from the cross-sectional estimated change for some measures (figure 3). Most striking of

Table 2 Number of measures and follow-up time for participants with at least 2 visits

	Total	Follow-up time, y, mean (SD)	Participants with 2/3/4/≥5 assessments
CSF $A\beta_{42}$	121	2.44 (0.96)	86/24/5/6
CSF tau	120	2.43 (0.96)	85/24/5/6
CSF p-tau_{181}	121	2.44 (0.96)	86/24/6/5
Cortical amyloid PiB	154	2.70 (1.08)	118/23/8/5
Hippocampal volume	133	2.59 (1.14)	104/16/9/4
FDG precuneus	170	2.64 (1.09)	128/25/13/4
DIAN cognitive composite	200	2.72 (1.07)	140/35/14/11
CDR sum of boxes	217	2.71 (1.09)	150/36/18/13

Abbreviations: Aβ = β-amyloid; CDR = Clinical Dementia Rating scale; DIAN = Dominantly Inherited Alzheimer Network; FDG = fluorodeoxyglucose; p-tau = phosphorylated tau; PiB = Pittsburgh compound B.

Figure 2 Model estimated individual rate of change for all imaging, CSF, and clinical measures over estimated year to symptom onset (EYO) for mutation carriers and noncarriers

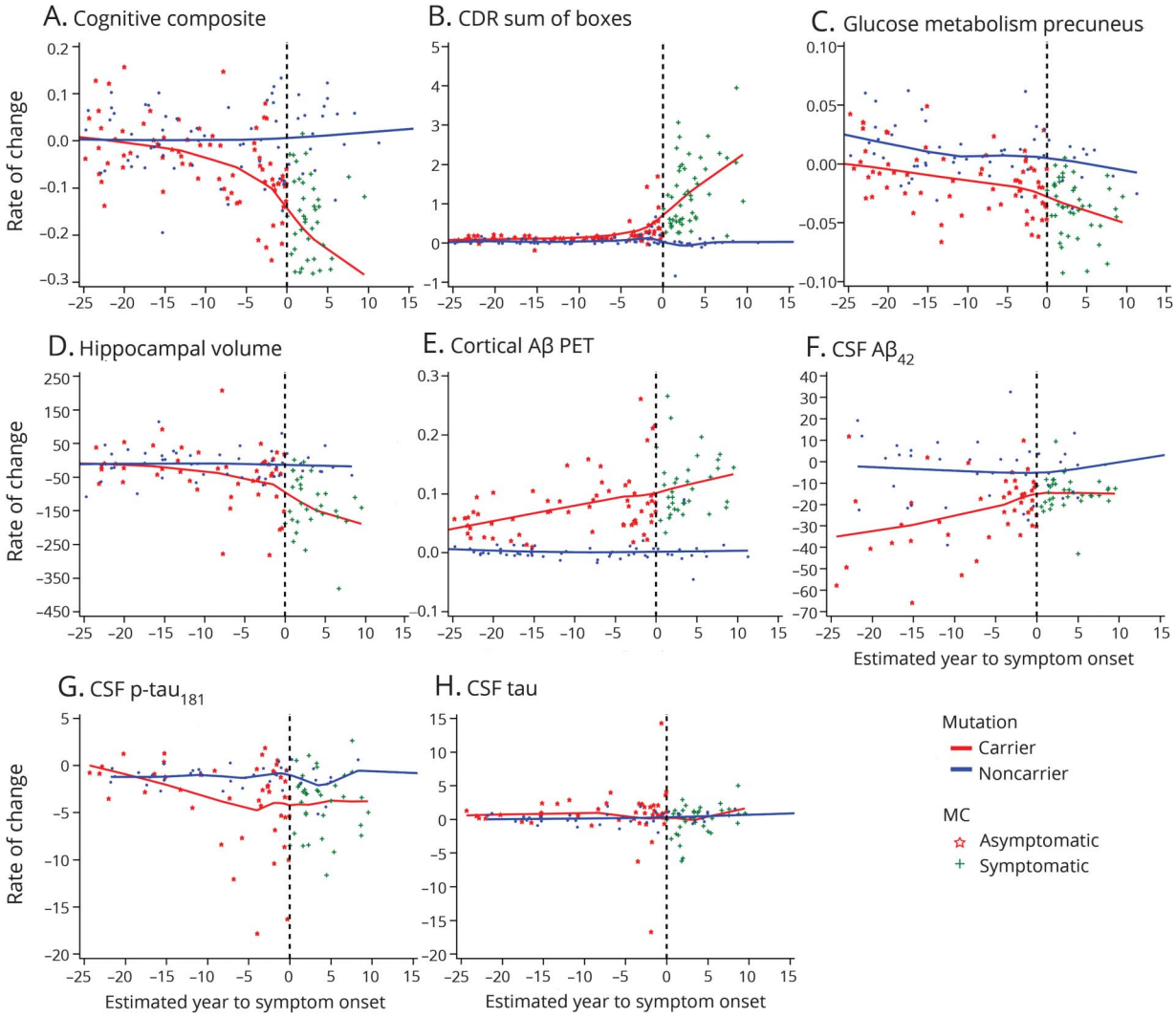

(A–H) Each point represents an individual's model estimated rate of change with their baseline EYO at the time of study entry. For each individual, the annualized rate of change is estimated in the units of measurement for each variable. The solid lines represent the LOESS for mutation carriers (red) and noncarriers (blue). Aβ = β-amyloid; CDR = Clinical Dementia Rating scale; p-tau = phosphorylated tau.

these were the differences demonstrated in CSF tau and p-tau; whereas the cross-sectional estimates showed a large increase over EYO in MCs, the longitudinal estimates suggested only a modest increase in CSF tau and mostly negative rates of change for CSF p-tau.

Discussion

Identifying the neurodegenerative cascade in AD is critical to better understand the underlying biology and developing therapies to modify the disease trajectory. An advantage of ADAD is disease predictability, thus allowing participants who enroll at different stages of disease to be combined to model disease progression over decades.[1,3,19] Based on comprehensive longitudinal data in the DIAN population, we find a period of approximately 25 years where critical changes in AD biomarkers emerge, including (1) the onset of Aβ-related changes, starting at least 25 years before anticipated symptom onset; (2) the onset of significant changes in markers of neuronal function (i.e., precuneus metabolism) beginning approximately 17 years before anticipated symptom onset; and (3) evidence of significant neuronal functional decline (i.e., decline in cognition and accelerated hippocampal atrophy) approximately 5 years before anticipated symptom onset with a dramatic decline in CSF p-tau$_{181}$. Importantly, these data describing within-participant changes in biomarkers offer the most comprehensive understanding of the pathobiology of ADAD to date. The results provide critical information necessary for pathology-specific prevention efforts and suggest optimal enrollment windows for targeting disease stage in ADAD (e.g., primary vs secondary vs tertiary prevention), and possibly LOAD.

Table 3 Rate of change estimates for asymptomatic only and asymptomatic and symptomatic mutation carriers combined

	Asymptomatic only			Asymptomatic and symptomatic		
Effect	**Estimate**	**Standard error**	***pr*** **> |t|**	**Estimate**	**Standard error**	***pr*** **> |t|**
FDG (SUVR)						
Time, y, MC	−0.030	0.010	0.0046	−0.039	0.007	<0.0001
Time, y, NC	0.005	0.014	0.7284	0.004	0.009	0.66
Time × baseline EYO MC	−0.001	<0.001	0.0153	−0.002	<0.001	<0.0001
Time × baseline EYO NC	<-0.001	<0.001	0.4191	−0.001	<0.001	0.05
Tau, ng/mL						
Time, y, MC	1.35	1.30	0.3061	0.49	0.99	0.62
Time, y, NC	−0.17	1.62	0.9157	0.20	1.28	0.87
p-tau, ng/mL						
Time, y, MC	3.49	3.30	0.2922	1.13	2.5	0.65
Time, y, NC	−2.23	4.08	0.5852	−3.0	3.5	0.40
Time × baseline EYO MC	0.21	0.20	0.2969	0.09	0.20	0.64
Time × baseline EYO NC	−0.04	0.26	0.8525	−0.09	0.26	0.73
Rate after change point MC	−1.31	0.60	0.0331	−0.71	0.32	0.03
Rate after change point NC	0.12	0.77	0.8703	0.24	0.38	0.54
PiB, SUVR						
Time, y, MC	0.10	0.018	<0.0001	0.083	0.014	<0.001
Time, y, NC	0.007	0.026	0.7743	−0.002	0.017	0.89
Time × baseline EYO MC	0.001	0.001	0.1291	0.001	0.001	0.51
Time × baseline EYO NC	<0.000	0.001	0.8728	−0.002	0.017	0.87
CDR sum of boxes						
Time, y, MC	0.36	0.074	<0.0001	0.45	0.13	0.01
Time, y, NC	0.15	0.096	0.1259	0.08	0.18	0.62
Time × baseline EYO MC	0.01	0.004	0.0003	0.023	0.009	0.02
Time × baseline EYO NC	0.007	0.006	0.2194	0.004	0.73	0.98
Composite (*z* score)						
Time, y, MC	−0.036	0.043	0.3985	−0.063	0.040	0.12
Time, y, NC	−0.045	0.057	0.4347	−0.008	0.047	0.86
Time × baseline EYO MC	−0.002	0.002	0.3466	−0.004	0.002	0.14
Time × baseline EYO NC	−0.002	0.003	0.5287	< −0.001	0.003	0.99
Rate after change point MC	−0.048	0.021	0.0264	−0.023	0.008	0.005
Rate after change point NC	0.011	0.025	0.6804	0.004	0.007	0.53
MRI (hippocampal vol mm^3), %[a]						
Time, y, MC	−1.35	0.45	0.0056	−1.0	0.6	0.008
Time, y, NC	−0.24	0.57	0.6745	−0.3	0.7	0.69
Time × baseline EYO MC	−0.056	0.033	0.0853	−0.04	0.04	0.29

Continued

Table 3 Rate of change estimates for asymptomatic only and asymptomatic and symptomatic mutation carriers combined *(continued)*

	Asymptomatic only			Asymptomatic and symptomatic		
Effect	**Estimate**	**Standard error**	***pr*** **> |t|**	**Estimate**	**Standard error**	***pr*** **> |t|**
Time × baseline EYO NC	−0.004	0.034	0.8956	−0.01	0.04	0.86
Ab42, ng/mL, %[b]						
Time, y, MC	−2.44	1.39	0.0896	−2.7	0.8	0.008
Time, y, NC	−2.81	2.22	0.2169	−0.5	1.0	0.62
Time × baseline EYO MC	0.26	0.12	0.0344	0.2	0.08	0.004
Time × baseline EYO NC	−0.14	0.16	0.3938	0.04	0.08	0.58

Abbreviations: CDR = Clinical Dementia Rating scale; EYO = estimated years to symptom onset; FDG = fluorodeoxyglucose; MC = mutation carrier; NC = mutation noncarrier; p-tau = phosphorylated tau; PiB = Pittsburgh compound B; SUVR = standardized uptake value ratio.
Cognitive composite *z* score/y; CSF tau and p-tau (pg/mL/y); FDG and PiB PET (SUVR/y).
[a] The mean for NC is 4,366, which was used to calculate the percent change.
[b] The mean for NC is 530, which was used to calculate the percent change.

Based on the longitudinal data, we identified important differences in the rates and patterns of progression[1,3,23] compared with cross-sectional based estimates. First, we show that the time period between initial increase in aggregated Aβ and accelerations in other biomarkers may occur at different intervals than those previously reported,[1,24] including earlier changes in precuneus metabolism and, possibly, elevated CSF p-tau (table 2). Further, the longitudinal estimates for some of the biomarkers indicated a more rapid change (e.g., FDG, CSF Aβ42, and p-tau$_{181}$) than predicted from cross-sectional estimates, an important consideration for interventional trial design, particularly in prevention trials aimed at trying to intervene prior to the change point in specific biomarker and clinical measures. Our findings of CSF Aβ42 and PiB-PET (fibrillar plaques) beginning to change at nearly the same time differs from some reports from non-ADAD where either measure has been demonstrated to change first.[25,26] Yet one such study in ADNI using the same xMAP-AlzBio3 assay for CSF Aβ1-42 found similar levels of Aβ1-42 in PiB-negative elderly participants[25] as the NC in DIAN. This highlights the importance of also exploring longitudinal changes in order to determine the point when abnormal changes begin. Differences in populations and measurements (amyloid radiotracers and CSF) and reference regions will likely contribute to relative differences in the timing of when biomarkers change. Nonetheless, this and work in LOAD confirms that both populations demonstrate nearly the same temporal ordering of amyloid changes first, followed by other non-Aβ biomarkers.

Table 4 Ordering of outcomes by estimated years to symptom onset (EYO) point where significantly different rates of change and where significant differences in the means of each outcome at baseline were identified between mutation carriers (MC) and noncarriers (NC)

		Longitudinal estimates		Cross-sectional estimates	
Outcome	**Mean (SD) of NCs[a]**	**EYO**	**Difference in the rate of change (MC − NC), mean, %**	**EYO**	**Difference in the mean at baseline (MC − NC), mean, %**
CSF Aβ42	530 (141)	−24	−6.2	−10	−15.7
PiB PET	1.1 (0.19)	−25	5.9	−22	23.6
FDG	1.9 (0.16)	−17	−1.16	−14	−2.52
CSF tau	47.7 (16.0)	NA		−14	47.2
Cognitive composite		−2	−0.1	−3	−0.33
Hippocampal volume, mm^3	4,366 (390)	−1	−1.6	0	−4.0
CSF p-tau	20.7 (6.6)	1	−15.9	−11	69.6
CDR sum of boxes		0	0.64	0	0.72

Abbreviations: Aβ = β-amyloid; CDR = Clinical Dementia Rating; FDG = fluorodeoxyglucose; p-tau = phosphorylated tau; PiB = Pittsburgh compound B.
[a] The mean of NCs for each outcome was used to convert the difference into percentage.

Figure 3 Comparison of cross-sectional and longitudinal estimated rates of change for imaging, CSF, and clinical measures in mutation carriers over estimated year to symptom onset (EYO)

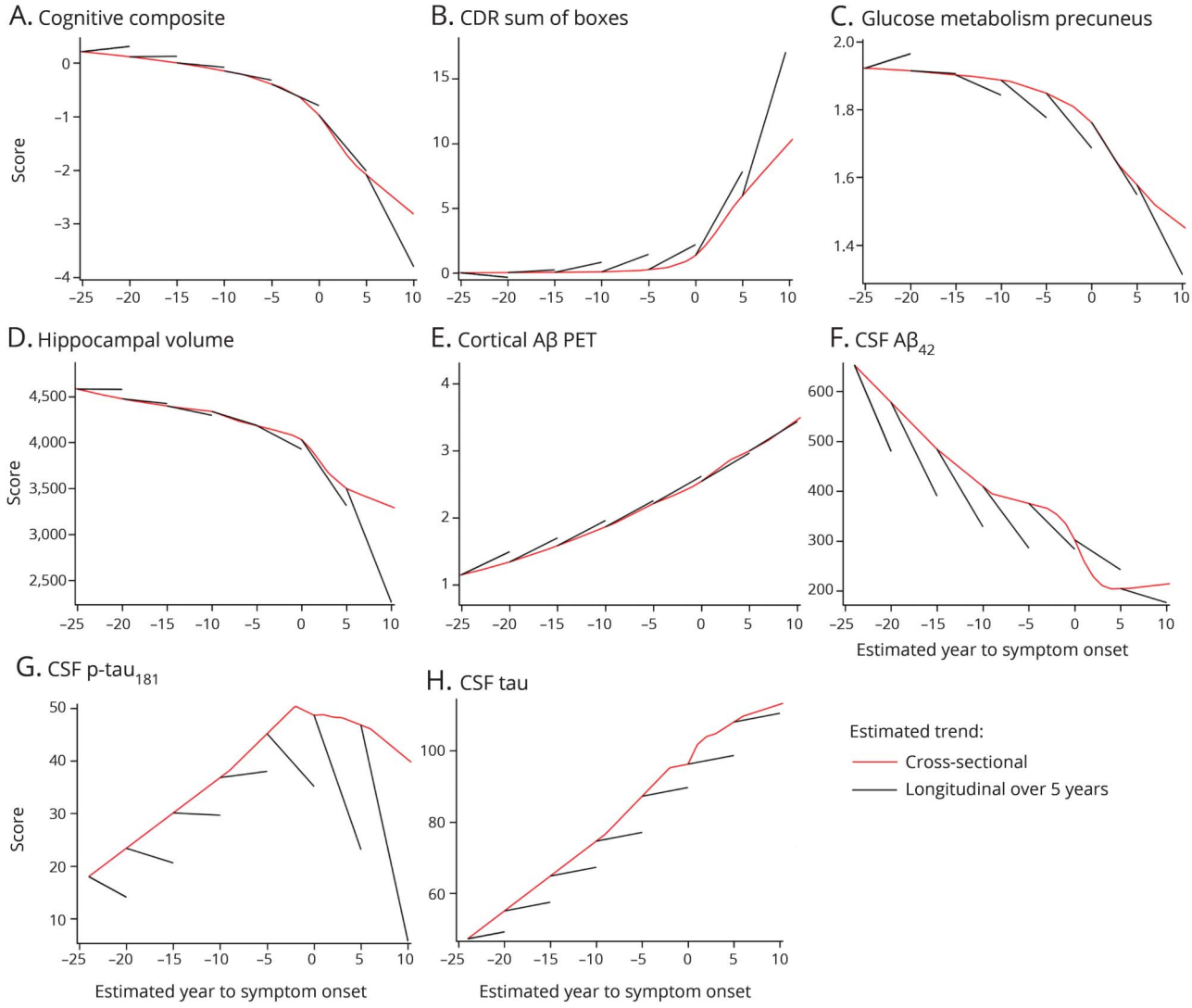

Clinical, cognitive, and biomarker measures across baseline EYO based on cross-sectional estimates (red line) and 5-year calculated longitudinal trajectories (black line) modeled from the longitudinal data. The longitudinal trajectory is estimated using the rate of change from the mixed effects model over the 5 years. These findings indicate consistent cross-sectional estimates with longitudinal confirmation for Pittsburgh compound B PET; however, in other measures, cross-sectional data underestimate the rate of change measured by longitudinal measures, with rapid changes noted in clinical measures, CSF tau, and brain atrophy. Aβ = β-amyloid; CDR = Clinical Dementia Rating scale; p-tau = phosphorylated tau.

Second, we found that the pattern of longitudinal increases in soluble CSF tau peptides was unexpectedly modest when modeled across the disease spectrum (figure 2, G and H). This is, in part, a result of the statistical method used, which estimates change based on the entire population. The result is that the large decline in CSF p-tau for the symptomatic population influences the overall estimates across the disease spectrum. It is clear that for total tau and p-tau, the MC group has significantly higher absolute levels than NCs between 15 and 10 years before anticipated symptom onset. Yet, the rate of change for both measures in the CDR 0 group only (table 3) demonstrated an increase of nearly 3 times the annual estimated change compared to the entire cohort. Further, we confirmed previous findings in the DIAN population that CSF p-tau decreases significantly as symptom onset approaches.[27] One possible explanation for this decline is the spread of neurofibrillary tangle (NFT) pathology and the subsequent sequestration of soluble p-tau, as suggested in transgenic animal studies[28]; this finding is similar to the dynamics of soluble and fibrillar Aβ[29] previously identified. This may also explain why the largest decline in p-tau appears to occur relatively close to the onset of clinical symptoms, as postmortem studies have consistently linked NFT burden to the degree of cognitive impairment. Work in LOAD has suggested that CSF tau levels may decline with disease progression, but the changes in p-tau identified here have not yet been reported.[30] There may be nonbiological contributions to the CSF tau findings, including small numbers of participants

at the extremes of EYO and limitations of the method used in this study to measure the soluble tau peptides (i.e., larger variance for both soluble tau measures compared to other variables, which limits the precision of the measurement to detect consistent intraindividual changes over time). The multisite nature of DIAN could contribute to CSF variability, but we found similar results when we restricted the assessment to a single site with the largest number of samples. Further, a recent study in ADNI reports the same direction of within-person longitudinal change in these markers in individuals diagnosed with LOAD.[31] To address this, more participants and alternative measurement techniques will likely be required.

Third, the longitudinal estimates also provide a refinement of the trajectories of biomarker changes in ADAD and help to better understand how each might be related to the other and to disease progression. For instance, in this population, the development of fibrillar Aβ pathology, once started, appears to continue to accumulate in a relatively linear fashion and preceded others. Importantly, the rates of increase of cortical PiB in the DIAN population are similar to those identified in non-ADAD populations in a number of recent studies using PiB (0.04–0.06 SUVr/year,[24] and Jack et al.,[32] 0.05–0.10 in the dynamic phase). However, we found evidence of a nonlinear pattern with some other biomarkers appearing to plateau (e.g., CSF Aβ and tau peptides), whereas in others, there was a slower change towards a threshold, followed by a more rapid acceleration of abnormality (e.g., hippocampal volumes and cognition). This suggests that if amyloid pathology triggers other pathologies of the disease, the relationship is not a linear one, and that once a certain threshold (e.g., of amyloid burden) is exceeded, the subsequent rate of change of other biomarkers (i.e., CSF p-tau) may become autonomous and more difficult to predict how further changes in amyloid pathology will relate to further changes in nonamyloid pathologies. Similarly, predicting how lowering amyloid plaque levels will affect other biomarkers and disease progression once the pathologic thresholds have been exceeded will be challenging. This also suggests that in the case of amyloid targeting therapies, identifying the burden of amyloid pathology where other (nonamyloid) biomarkers begin to change may be critical to identifying the point of maximal benefit, rather than focusing on the levels typically separating disease vs nondisease.

Limitations of this study include different missing data for various measures, which may influence the accuracy of each estimate. However, only approximately 15% of participants with missing data had missing data from more than one class of biomarkers (e.g., CSF and imaging), thus measures of a particular pathology (i.e., Aβ or neurodegeneration) are still captured in the majority of participants. A further limitation in models that estimate change is that the model itself may introduce bias. However, the LOESS fit for the model estimated data are consistent with actual data in figure 1, indicating there is little effect of model bias. In support of robust findings, a recent publication focusing exclusively on the longitudinal imaging measures but using a different Bayesian statistical approach found results similar to ours.[33] Our choice of reference region for PET may have effects on the outcomes. However, we have recently performed an analysis in the DIAN population that compared results of longitudinal PiB when using different reference regions with and without partial volume correction[21] and found partial volume correction to be the most important determinant for longitudinal analyses. Further, our recent publication of longitudinal imaging in DIAN found no significant differences on the results when comparing different reference regions.[33] Finally, our results are dependent on the accuracy of the DIAN EYO, which is strongly associated with individual age at onset across multiple mutations.[13] Future collection of prospective disease onset will likely improve the DIAN EYO.

Recent cross-sectional estimates of biomarker changes in the preclinical phases of ADAD and LOAD appear to support the sequence of biomarker changes based on longitudinal data from the DIAN study. However, important differences identified in this work provide the basis of a better understanding of the disease progression. Determining the period of time between initial Aβ pathology and neuronal dysfunction is critical in guiding future trials aimed at disease modification and prevention. These data suggest that the therapeutic window for disease prevention and modification may begin at least 20 years before the onset of dementia symptoms and, particularly in the case of a single therapeutic target (e.g., amyloid), may begin to close within a few years prior to cognitive decline.

Author contributions

E.M., G.W., B.A.G., J.H., C.X., R.J.B.: data analysis, literature search, study design, writing. E.M., V.B., A.M.F., A.M.G., D.S.M., J.C.M., R.A., S.B.B., W.K., J.N., J.R., B.G., M.R., R.A.S., J.C., S.S., N.R.G.-R., P.R.S., M.N.R., N.C.F., J.L., M.J., R.J.B.: data collection. B.A.G., T.L.S.B., V.B., D.H., N.J.C., A.M.F., A.M.G., D.S.M., J.C.M., R.A., S.B.B., W.K., J.N., J.R., B.G., M.R., R.A.S., J.C., S.S., N.R.G.-R., P.R.S., M.N.R., N.C.F., J.L., M.J., R.J.B.: critical analysis of manuscript.

Acknowledgment

This article has been reviewed by the DIAN study investigators for scientific content and consistency of data interpretation with previous DIAN study publications. The authors thank the participants and their families and contributions of the DIAN research and support staff at each of the participating sites for their contributions to this study. The DIAN Expanded Registry (dianxr.org) welcomes contact from any ADAD families or treating clinicians interested in research.

Study funding

Data collection and sharing for this project was supported by The Dominantly Inherited Alzheimer Network (DIAN, UF1 AG032438) funded by the National Institute on Aging (NIA), the German Center for Neurodegenerative Diseases

(DZNE), the Raul Carrea Institute for Neurological Research (FLENI), the MRC Dementias Platform UK (MR/L023784/1 and MR/009076/1), and NIHR Queen Square Dementia Biomedical Research Unit. This manuscript has been reviewed by DIAN Study investigators for scientific content and consistency of data interpretation with previous DIAN Study publications. The corresponding authors had full access to the data in the study and had final responsibility for the decision to submit for publication.

Disclosure

E. McDade: Elli Lilly scientific advisory board, UpToDate. G. Wang and B. Gordon report no disclosures relevant to the manuscript. J. Hassenstab: Biogen (consultant), Lundbeck (consultant). T. Benzinger and V. Buckles report no disclosures relevant to the manuscript. A. Fagan: Roche Diagnostics (advisory board), IBL international (advisory board), DiamiR (consultant), AbbVie (consultant), Genentech (advisory board). D. Holtzman and N. Gairnes report no disclosures relevant to the manuscript. A. Goate: royalties from Taconic and Athena Diagnostics; personal fees from Denali Therapeutics, AbbVie. D. Marcus, J. Morris, K. Paumier, C. Xiong, R. Allegri, and S. Berman report no disclosures relevant to the manuscript. W. Klunk: GE Healthcare holds a license agreement with the University of Pittsburgh based on the PiB PET technology described in this manuscript. Dr. Klunk is a coinventor of PiB and, as such, has a financial interest in this license agreement. GE Healthcare provided no grant support for this study and had no role in the design or interpretation of results or preparation of this manuscript. The other authors have no conflicts of interest based on PiB PET and had full access to all of the data in the study and take responsibility for the integrity of the data and the accuracy of the data analysis. J. Noble, J. Ringman, B. Ghetti, and M. Farlow report no disclosures relevant to the manuscript. R. Sperling: personal fees from Avid/Lilly, personal fees from Janssen Immunotherapy, personal fees from Bracket, personal fees from Genentech, personal fees from Sanofi, personal fees from Roche, personal fees from AbbVie, personal fees from Lundbeck, personal fees from Otsuka, personal fees from Merck, outside the submitted work. J. Chhatwal, S. Salloway, N. Graff-Radford, P. Schofield, C. Masters, and M. Rossor report no disclosures relevant to the manuscript. N. Fox: personal fees from Janssen, personal fees from Roche, personal fees from Lilly, personal fees from Novartis, personal fees from GSK, personal fees from Biogen, outside the submitted work and paid to UCL. J. Levin: personal fees from Aesku, personal fees from Bayer Vital, personal fees from Willi Gross Foundation, outside the submitted work. M. Jucker and R. Bateman report no disclosures relevant to the manuscript. Go to Neurology.org/N for full disclosures.

Publication history

Received by *Neurology* August 22, 2017. Accepted in final form July 5, 2018.

References

1. Bateman RJ, Xiong C, Benzinger TL, et al. Clinical and biomarker changes in dominantly inherited Alzheimer's disease. N Engl J Med 2012;367:795–804.
2. Mills SM, Mallmann J, Santacruz AM, et al. Preclinical trials in autosomal dominant AD: implementation of the DIAN-TU trial. Rev Neurol2013;169:737–743.
3. Fleisher AS, Chen K, Quiroz YT, et al. Associations between biomarkers and age in the presenilin 1 E280A autosomal dominant Alzheimer disease kindred: a cross-sectional study. JAMA Neurol 2015;72:316–324.
4. Fox NC, Warrington EK, Seiffer AL, Agnew SK, Rossor MN. Presymptomatic cognitive deficits in individuals at risk of familial Alzheimer's disease: a longitudinal prospective study. Brain 1998;121:1631–1639.
5. Reiman EM, Quiroz YT, Fleisher AS, et al. Brain imaging and fluid biomarker analysis in young adults at genetic risk for autosomal dominant Alzheimer's disease in the presenilin 1 E280A kindred: a case-control study. Lancet Neurol 2012;11:1048–1056.
6. Wallon D, Rousseau S, Rovelet-Lecrux A, et al. The French series of autosomal dominant early onset Alzheimer's disease cases: mutation spectrum and cerebrospinal fluid biomarkers. J Alzheimers Dis 2012;30:847–856.
7. Ringman JM, Younkin SG, Pratico D, et al. Biochemical markers in persons with preclinical familial Alzheimer disease. Neurology 2008;71:85–92.
8. Cash DM, Ridgway GR, Liang Y, et al. The pattern of atrophy in familial Alzheimer disease: volumetric MRI results from the DIAN study. Neurology 2013;81:1425–1433.
9. Chhatwal JP, Schultz AP, Johnson K, et al. Impaired default network functional connectivity in autosomal dominant Alzheimer disease. Neurology 2013;81:736–744.
10. Ringman JM, Liang LJ, Zhou Y, et al. Early behavioural changes in familial Alzheimer's disease in the Dominantly Inherited Alzheimer Network. Brain 2015;138:1036–1045.
11. Storandt M, Balota DA, Aschenbrenner AJ, Morris JC. Clinical and psychological characteristics of the initial cohort of the Dominantly Inherited Alzheimer Network (DIAN). Neuropsychology 2014;28:19–29.
12. Jack CR Jr, Holtzman DM. Biomarker modeling of Alzheimer's disease. Neuron 2013;80:1347–1358.
13. Ryman DC, Acosta-Baena N, Aisen PS, et al. Symptom onset in autosomal dominant Alzheimer disease: a systematic review and meta-analysis. Neurology 2014;83:253–260.
14. Sperling RA, Rentz DM, Johnson KA, et al. The A4 study: stopping AD before symptoms begin? Sci Transl Med 2014;6:228fs13.
15. Reiman EM, Langbaum JB, Fleisher AS, et al. Alzheimer's Prevention Initiative: a plan to accelerate the evaluation of presymptomatic treatments. J Alzheimers Dis 2011;26(suppl 3):321–329.
16. Morris JC, Aisen PS, Bateman RJ, et al. Developing an international network for Alzheimer research: the Dominantly Inherited Alzheimer Network. Clin Invest 2012;2:975–984.
17. Morris JC. The Clinical Dementia Rating (CDR): current version and scoring rules. Neurology 1993;43:2412–2414.
18. Bateman RJ, Benzinger TL, Berry S, et al. The DIAN-TU Next Generation Alzheimer's prevention trial: adaptive design and disease progression model. Alzheimers Dement 2017;13:8–19.
19. Benzinger TL, Blazey T, Jack CR Jr, et al. Regional variability of imaging biomarkers in autosomal dominant Alzheimer's disease. Proc Natl Acad Sci USA 2013;110:E4502–E4509.
20. Su Y, D'Angelo GM, Vlassenko AG, et al. Quantitative analysis of PiB-PET with FreeSurfer ROIs. PLoS One 2013;8:e73377.
21. Su Y, Blazey TM, Owen CJ, et al. Quantitative amyloid imaging in autosomal dominant Alzheimer's disease: results from the DIAN study group. PLoS One 2016;11:e0152082.
22. Cleveland WS, Devlin SJ, Grosse E. Regression by local fitting: methods, properties, and computational algorithms. J Econom 1988;37:87–114.
23. Jack CR, Wiste HJ, Weigand SD, et al. Amyloid-first and neurodegeneration-first profiles characterize incident amyloid PET positivity. Neurology 2013;81:1732–1740.
24. Villemagne VL, Burnham S, Bourgeat P, et al. Amyloid beta deposition, neurodegeneration, and cognitive decline in sporadic Alzheimer's disease: a prospective cohort study. Lancet Neurol 2013;12:357–367.
25. Palmqvist S, Mattsson N, Hansson O. Cerebrospinal fluid analysis detects cerebral amyloid-beta accumulation earlier than positron emission tomography. Brain 2016;139:1226–1236.
26. Palmqvist S, Schöll M, Strandberg O, et al. Earliest accumulation of β-amyloid occurs within the default-mode network and concurrently affects brain connectivity. Nat Commun 2017;8:1214.
27. Fagan AM, Xiong C, Jasielec MS, et al. Longitudinal change in CSF biomarkers in autosomal-dominant Alzheimer's disease. Sci Transl Med 2014;6:226ra30.
28. Yamada K, Cirrito JR, Stewart FR, et al. In vivo microdialysis reveals age-dependent decrease of brain interstitial fluid tau levels in P301S human tau transgenic mice. J Neurosci 2011;31:13110–13117.
29. Potter R, Patterson BW, Elbert DL, et al. Increased in vivo Amyloid-Beta 42 production, exchange, and irreversible loss in presenilin mutations carriers. Sci Transl Med 2013;5:189ra77.
30. Toledo JB, Xie SX, Trojanowski JQ, Shaw LM. Longitudinal change in CSF Tau and Aβ biomarkers for up to 48 months in ADNI. Acta Neuropathol 2013;126:659–670.
31. Sutphen CLML, Herries EM, Xiong C, Ladenson JH, Holtzman DM, Fagan AM. Longitudinal decrease in multiple cerebrospinal fluid biomarkers of neuronal injury in symptomatic late onset Alzheimer disease. Alzheimers Dement 2018;14:869–879.
32. Jack CR, Wiste HJ, Knopman DS, et al. Rates of beta-amyloid accumulation are independent of hippocampal neurodegeneration. Neurology 2014;82:1605–1612.
33. Gordon BA, Blazey TM, Su Y, et al. Spatial patterns of neuroimaging biomarker change in individuals from families with autosomal dominant Alzheimer's disease: a longitudinal study. Lancet Neurol 2018;17:241–250.